

Mathematical Model for the Unidirectional Solidification of Metals: II. Massive Molds

A. GARCIA, T. W. CLYNE, AND M. PRATES

In this paper, a new mathematical model recently outlined by the present authors¹ is applied to the case of unidirectional solidification via heat extraction through massive uncooled molds of effectively semi-infinite thickness. The model permits measurement of the Newtonian heat transfer coefficient at the metal/mold interface and a complete description of the kinetics and thermal characteristics of solidification is subsequently possible. Experimental results are compared with predictions for the case of lead and the effect of mold thickness in the effectively finite regime is also investigated.

THE mathematical treatment of the generalized unidirectional solidification problem presents considerable complexity and exact solutions are available for only a few restricted cases. The basic mathematical obstacle to analysis is the simultaneous treatment of heat flow through metal and/or mold by thermal conduction and across the metal/mold interface by Newtonian heat transfer. The only generalized solutions which place no restriction on the interfacial heat transfer coefficient are those utilizing mathematical approximations.²⁻⁶

The proposed model utilizes a novel approach to the heat flow problem. A basic assumption is that the heat transfer coefficient remains constant during the solidification process.* The thermal resistance

*Physically, this may be approximately valid in some situations but not in others. The formation of an 'air gap' between metal and mold as a result of contraction has frequently been postulated⁷⁻⁹ as a mechanism for a time dependence of h_i (or a position dependence in a steady state process such as continuous casting). In practice, the importance of this probably depends on metal, mold surface, geometry and so forth; in the experimental set-up used in this study, changes of h_i with time would be expected to be small and this supported by the internal consistency of experimental measurements both in this study and in the previous one. Mathematically, the case of variable h_i is certainly not treatable by exact analytical methods.

presented by the interface is then modeled by a "pre-existing" thickness of solid, which, for the purposes of heat flow calculations, is additive to the real physical thickness. Heat flow may then be completely described by manipulation of the basic Fourier conduction equations.

For the previously described case¹ of a thin, highly refrigerated mold, where heat flow in the metal only need be treated, it was necessary simply to introduce a presolidified thickness of metal to represent the interface resistance. In the present more general case, heat flow in both metal and mold are significant; a virtual thickness of each must be postulated to account for interface resistance which is divided into two components separated by a hypothetical plane of constant temperature (in accordance with the normal approaches to this problem).^{10,11} Temperatures of metal and mold at the interface are then permitted to vary (approach the temperature of the hypothetical

plane) in a way determined by the characteristics of the heat flow.

Theoretical predictions are compared with experiment for solidification of lead both with and without an insulating layer coated on to the mold face. The deviation from theory introduced by a finite mold thickness is also investigated.

MATHEMATICAL MODEL

The basic assumptions of the model are similar to those presented in the previous paper¹ (and, indeed, to those generally assumed when treating the kinetics of unidirectional solidification).^{2,5,12-14} They are:

- 1) Conductive heat flow is unidimensional,
- 2) The Newtonian interface resistance is represented by a heat transfer coefficient, h_i , which remains constant throughout the process,
- 3) The metal freezes with a macroscopically plane solid/liquid interface and at a congruent temperature, T_f ,
- 4) Superheat is assumed negligible and spurious heat losses from the liquid, by convection and radiation, are small,
- 5) Thermal properties of metal and mold are independent of both position and time.

The heat flow is now treated in two regimes, connected by the hypothetical plane of constant temperature. In both these components, a virtual system is set up in which the Newtonian resistance is represented by a pre-existing adjunct of material. (The two virtual systems produced in this way are actually equivalent except for a change of origin). The subdivision of the real system into two components and the derivation of the virtual systems is illustrated in Fig. 1. It is important to note that in the rest of this analysis, heat flow for the two components of the system are treated independently (being linked only by equality of heat flux across and temperature at the hypothetical plane) so that the difference in selected origin for the two virtual systems will introduce no error. The parameter x' is therefore used to denote position in both virtual systems. An outline of the meaning of all the symbols used in the analysis is given in Appendix I.

The relationships between parameters in the real and virtual systems are identical to those outlined in the first paper,¹ with the addition that x' is given by $(x - E_0)$ in the mold component. The Fourier field

A. GARCIA, T. W. CLYNE, and M. PRATES are Professors at the Department of Mechanical Engineering, State University of Campinas (UNICAMP), Campinas, SP, Brazil.

Manuscript submitted June 30, 1978.

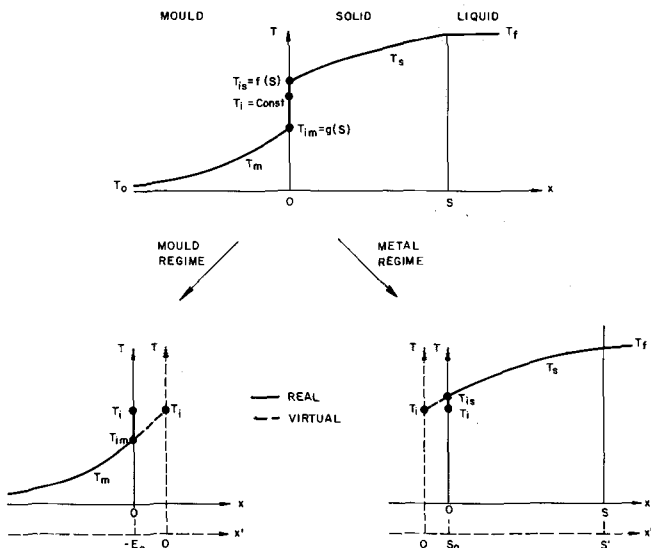


Fig. 1—Division of system into mold and metal components and relationship between real and virtual systems in these regimes.

equation is now valid between appropriate limits in both components, and has the general solution:

$$T = A + B \operatorname{erf} \left(\frac{x'}{2\sqrt{at'}} \right) \quad [1]$$

i) Solidification Time and Rate

By applying the boundary condition $T = T_f = \text{constant}$ at the liquid/solid interface and putting the argument of the error function in the solution to the Fourier equation equal to the constant ϕ for this case, it is simple to show¹ that:

$$t = \frac{S^2}{4a_s\phi^2} + \frac{S_0S}{2a_s\phi^2} \quad [2]$$

which describes the kinetic behavior in terms of the constants ϕ and S_0 which will shortly be defined.

ii) Thermal Profile

a) **Metal Component.** Applying the boundary condition $T = T_i = \text{constant}$ at the metal/mold interface, together with the previously mentioned condition at the liquid/solid interface, the constants of the solution of Eq. [1] for the profile in the metal can be written down immediately; it follows from the definition of ϕ that:

$$T_s = T_i + \frac{(T_f - T_i)}{\operatorname{erf}(\phi)} \operatorname{erf} \left(\phi \frac{S_0 + x}{S_0 + S} \right) \quad [3]$$

and substitution of $x = 0$ will give the metal temperature at the metal/mold interface, T_{is} , which will clearly tend to T_i as S becomes large.

b) **Mold Component.** Applying the boundary condition $T = T_0 = \text{constant}$ remote from the metal/mold interface ($x' = -\infty$), together with the previously mentioned condition at this interface, the constants in the general Eq. [1] are seen in this case to be:

$$A_m = T_i \quad [4a]$$

$$B_m = T_i - T_0 \quad [4b]$$

Now, because of the identity:

$$\frac{x'}{2\sqrt{a_m t'}} = \phi \frac{x'}{S'} \sqrt{a_s/a_m} = N\phi \frac{x'}{S'} \quad [5a]$$

where

$$N = \sqrt{a_s/a_m} \quad [5b]$$

the general solution is given by:

$$T_m = T_i + (T_i - T_0) \operatorname{erf} \left[N\phi \frac{(x - E_0)}{(S_0 + S)} \right] \quad [6]$$

Substitution of $x = 0$ in this equation will give the mold temperature at the mold/metal interface, T_{im} , which will tend to T_i as S becomes large.

iii) Determination of T_i

Applying the boundary condition of identity of heat flux from metal regime to mold regime across the hypothetical plane and obtaining the appropriate gradients by differentiating Eqs. [3] and [6], on substitution we have:

$$k_m(T_i - T_0)N = k_s \frac{(T_f - T_i)}{\operatorname{erf}(\phi)} \quad [7]$$

which can be rearranged to give an expression for T_i :

$$T_i = T_0 + \frac{(T_f - T_0)M}{M + \operatorname{erf}(\phi)} \quad [8a]$$

where

$$M = \sqrt{k_s d_s c_s / k_m d_m c_m} \quad [8b]$$

iv) Determination of ϕ

A thermal balance is applied at the liquid/solid interface, with the thermal gradient obtained by differentiating Eq. [3] evaluated at $x' = S'$. The interface velocity is simply obtained by differentiating Eq. [2] and the condition then reduces to:

$$\sqrt{\pi} \phi \exp(\phi^2) \operatorname{erf}(\phi) = \frac{c_s(T_f - T_i)}{H} \quad [9a]$$

The interval $(T_f - T_i)$ may be related to the known constant $(T_f - T_0)$ by manipulation of Eq. [8a], so that Eq. [9a] may be written in the form:

$$\sqrt{\pi} \phi \exp(\phi^2) [M + \operatorname{erf}(\phi)] = \frac{c_s(T_f - T_0)}{H} \quad [9b]$$

from which the constant ϕ may be obtained by iteration for any given metal/mold combination. Figure 2 illustrates the dependence of ϕ on M (the ratio of heat diffusivities of metal and mold) and $1/H^*$ (ratio of heat content of solid metal at freezing interface to latent heat of fusion).

v) Determination of S_0

The heat transfer across the metal/mold interface is handled by the introduction of two partial heat transfer coefficients, h_{is} and h_{im} , referring to metal and mold components respectively (in accordance with usual practice in treating this case). Applying a thermal balance at the real metal/mold interface on the metal side:

$$h_{is}(T_{is} - T_i) = k_s \left(\frac{\partial T_s}{\partial x'} \right)_{x'=S_o} \quad [10a]$$

and applying this equation at $t = 0$ ($t' = t_o$), the boundary condition $T_{is} = T_f$ when $S' = S_o$ gives,

$$h_{is}(T_f - T_i) = k_s \left(\frac{\partial T_s}{\partial x'} \right)_{x'=S_o=S'} \quad [10b]$$

This thermal gradient is found by differentiating Eq. [3] and evaluating at $x' = S' = S_o$. After substitution and simplification (using Eq. [9b]) this leads to:

$$S_o = \frac{2a_s \phi^2 H d_s [M + \text{erf}(\phi)]}{h_{is}(T_f - T_o) \text{erf}(\phi)} \quad [11]$$

so that S_o is determined in terms of h_{is} (shortly to be defined) and properties of metal and mold.

vi) Determination of E_o

A similar balance is made to the above, this time on the mold side of the metal/mold interface:

$$h_{im}(T_i - T_{im}) = k_m \left(\frac{\partial T_m}{\partial x'} \right)_{x'=-E_o} \quad [12a]$$

which, applied at $t = 0$ ($t' = t_o$), when $T_{im} = T_o$ and $S' = S_o$ gives:

$$h_{im}(T_i - T_o) = k_m \left(\frac{\partial T_m}{\partial x'} \right)_{x'=-E_o, S'=S_o} \quad [12b]$$

This thermal gradient is found by differentiating Eq. [6] and evaluating at $x' = -E_o$ and $S' = S_o$. Substitution and simplification gives:

$$E_o = \frac{S_o}{N\phi} \sqrt{\ln \left(\frac{2N\phi k_m}{\sqrt{\pi} h_{im} S_o} \right)} \quad [13]$$

vii) Determination of h_{is} and h_{im}

Identity of heat flux across both components and across the combined composite requires that:

$$\frac{h_{is}}{h_{im}} = \frac{(T_i - T_o)}{(T_f - T_i)} \quad [14a]$$

$$\frac{h_i}{h_{im}} = \frac{(T_i - T_o)}{(T_f - T_o)} \quad [14b]$$

and by substitution from Eq. [8], it follows that:

$$h_{im} = \left[1 + \frac{\text{erf}(\phi)}{M} \right] h_i \quad [15a]$$

$$h_{is} = \left[1 + \frac{M}{\text{erf}(\phi)} \right] h_i \quad [15b]$$

vii) Dimensionless Form of Model

The kinetics of the solidification process have now been completely described. The dependence of interface position (and velocity) on time is defined by Eq. [2] in terms of ϕ and S_o . Equation [9] fixes ϕ and Eq. [11] defines S_o in terms of h_{is} , which is related to h_i by Eq. [15b]. Similarly, the thermal profiles in metal

and mold at any time are given by Eqs. [3] and [6], which are now completely defined for a given metal/mold combination and remain only to be specified in terms of h_i . The value of h_i for any particular case will depend on the details of surface finish and so forth and can be extracted from the literature for specified conditions or may be obtained experimentally. In this study, h_i was found by experimental measurements of the dependence of thickness solidified on time, the details of which are described below.

The relationship between time and thickness solidified, represented by Eq. [2], may be presented in terms of dimensionless parameters:

$$t^* = \left(\frac{S_o^*}{2\phi} \right)^2 + H^* S_o^* \quad [16]$$

Also, the thermal profiles represented by Eqs. [3] and [6] may be more conveniently given in the dimensionless forms shown below:

$$T_s^* = \frac{T_s - T_o}{T_f - T_o} = \frac{M + \text{erf}(\phi) \frac{S_o^* + x^*}{S_o^* + S_o^*}}{M + \text{erf}(\phi)} \quad [17a]$$

$$T_m^* = \frac{T_m - T_o}{T_f - T_o} = \frac{M}{M + \text{erf}(\phi)} \left[1 + \text{erf} \left(\frac{\phi}{M} \cdot \frac{x^* - E_o^*}{S_o^* + S_o^*} \right) \right] \quad [17b]$$

where all the dimensionless parameters are defined in Appendix I.

EXPERIMENTAL AND DISCUSSION

The experimental examination of this case under the specified conditions is rather more difficult than that of the cooled mold due to the problem of bringing metal and mold into initial contact. It was not possible to bring the liquid into thermal equilibrium within the ingot before initiating cooling, as was done for the cooled molds,¹ and in this case it was necessary to pour liquid (with a very low superheat of $\sim 3^\circ\text{C}$) directly into the mold, the lateral walls of which were close to the freezing temperature and heat-extracting block close to ambient temperature. Thermal data during solidification were obtained through a number of fine thermocouples accurately positioned with respect to the heat extracting surface, locations of the freezing interface being determined via the output of those in the solidifying metal. This was carried out for the freezing of lead (purity ~ 99.9 pct) with two different interfacial heat transfer conditions corresponding to the heat-extracting surface being a) polished and b) painted with a thin ($\sim 100 \mu\text{m}$) alumina coating by means of a spray gun. The molds used were of low alloy steel (En 27) and wall thicknesses of 100 mm (semi-infinite*), 40, 30, 15 and 5 mm were used, the

*That this thickness closely corresponded to the semi-infinite case was confirmed by various thermal data from metal and mold; see below.

thickness of metal to be solidified always being 50 to 60 mm. In all cases, unidirectionality of heat flow was confirmed by macrostructural examination, a typical grain structure being that shown in Fig. 3. (Only with the thinnest wall thickness was noticeable loss of directionality observed.) For the semi-infinite mold case, the experimental results for variation of

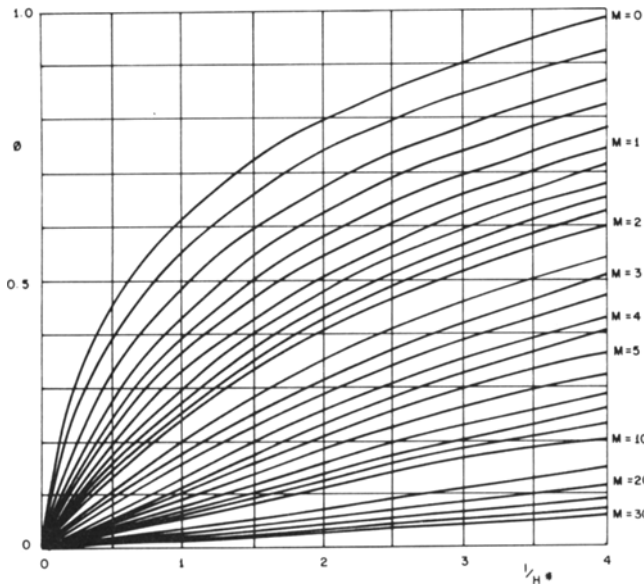


Fig. 2—Graphical solution of Eq. [9b] through which the solidification constant ϕ for the semi-infinite mold case is determined from thermal properties of metal and mold.

thickness with time are shown in Fig. 4 for the two thermal contact conditions.

The heat transfer coefficient h_i is obtained for any individual case by experimental measurements of thickness solidified. It is clear that Eq. [2] can be written in the form:

$$\frac{t}{S} = \alpha S + \beta \quad [18]$$

where α and β are constants defined in terms of ϕ and

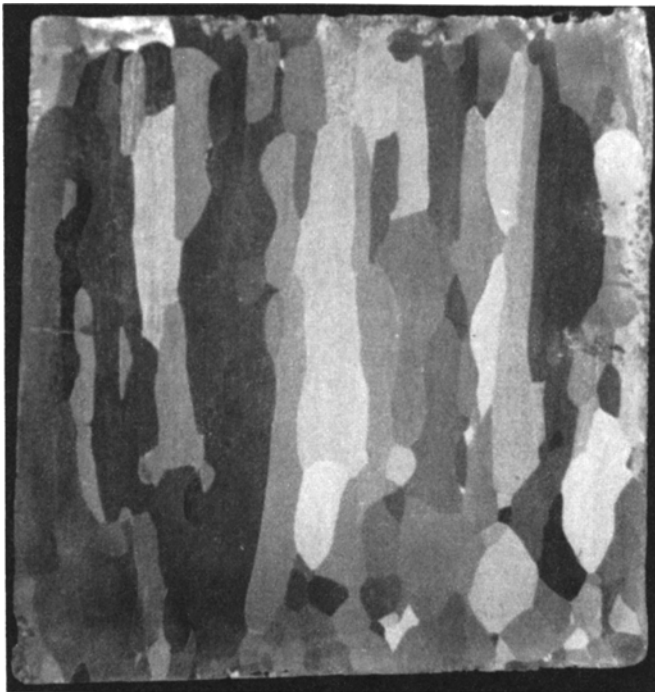


Fig. 3—Longitudinal macrostructure of lead unidirectionally solidified from a mold of thickness 40 mm.

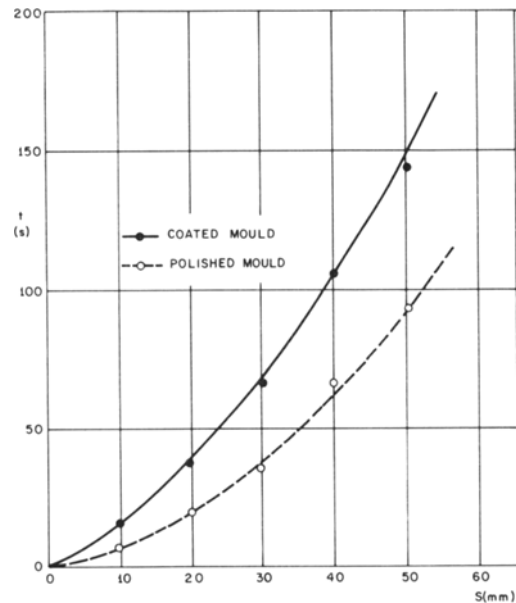


Fig. 4—Experimental results for variation of position of freezing interface with time during solidification of lead against a semi-infinite mold.

S_o . However, by equating $h_i(T_f - T_o)$ to the heat flux leaving the metal when $x' = S' = S_o$ and substituting from Eq. [9], it is easily shown that h_i is given by:

$$h_i = \frac{k_s 2\phi^2 H}{c_s S_o (T_f - T_o)} \quad [19]$$

from which, referring to Eq. [2], it is clear that,

$$h_i = \frac{H d_s}{(T_f - T_o) \beta} \quad [20]$$

It follows that h_i may be simply obtained from experimental measurements of S with time presented in the form of a graph of t/S against S , the intercept of which will be β . It may be noted that Eq. [20] is identical to the one used in the previous paper¹ dealing with cooled molds— β for the two cases being equal (for the same metal/mold combination and surface condition) although the values of both ϕ and S_o will be different. This is as expected because the value of the heat transfer coefficient depends only on the nature of the interface. A graph of t/S against S is shown in Fig. 5 for the polished and coated surface cases, with the two extracted values of β indicated. It may be noted that the corresponding graph for the case of lead solidified in chilled molds with similar surfaces¹ gave very similar values of β^* (although the gradients of the

*In fact the value obtained for the polished surface is slightly greater in the present case, probably because the production of a high degree of polish was impeded by a rim on the mold block. The state of polish can have a significant effect on values of h_i .^{14,15}

lines, representing α , were different in this case). The value of h_i derived from these measured values of β for the two cases are shown in Table I. It may be pointed out that these figures agree quite well with values commonly quoted in the literature,^{4,15} for these materials with similarly treated mold surfaces.

For the purposes of comparison of theory with experiment, the constants of Eq. [16] were evaluated for the materials being used (from the data in Appendix II) and this gave the equation:

Table I. Values of Interfacial Heat Transfer Coefficients Obtained Through Eq. [32] from Values of β Extracted Graphically from Experimental Data for Cases Examined.

Metal	Mold	Mold Surface	β , s/cm ± 0.2	h_i , kJ/m ² Ks
Lead	Low Alloy Steel	Polished	2.2	4.2
Lead	Low Alloy Steel	Coated (100 μ m)	12.0	0.75

$$t^* = 0.72 S^{*2} + 0.60 S^* \quad [21]$$

which is shown as the solid curve in Fig. 6, together with the experimental points derived from both polished and coated mold cases. It can be seen that the agreement between theory and experiment is good over the complete range.

As a further check on the validity of the model, changes of temperature with time were examined at various points in the metal and mold and compared with the predictions of Eq. [17]. This necessitated evaluation of the complete set of constants involved in the model and the calculated values of these parameters are shown in Table II for the two mold surface conditions. Substituting these values into Eq. [17], a curve can be drawn of T_s^* or T_m^* against S^* for any given x^* . Two such curves are shown in Fig. 7 corresponding to $x^* = 0.26$ (in metal 10 mm from interface) for the coated mold and $x^* = -3.81$ (in mold 30 mm from interface) for the polished case, together with the experimental output of thermocouples located at these positions (combined with the appropriate curve in Fig. 4 to relate time to thickness solidified). It can be seen that the agreement between theory and experiment is good, particularly bearing in mind the

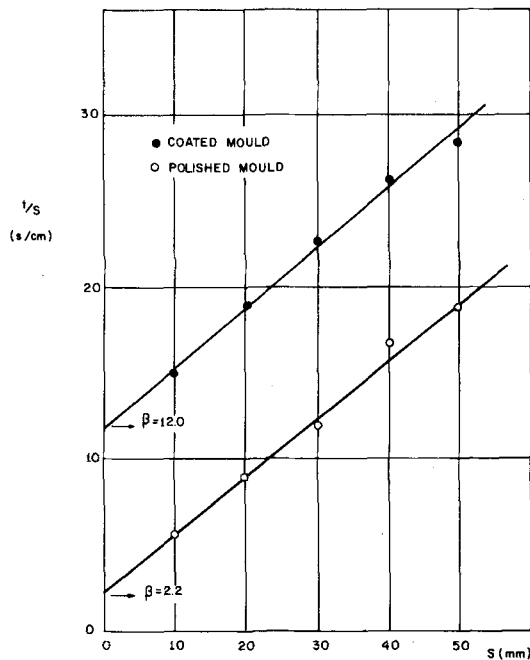


Fig. 5—Experimental measurements for polished and coated molds of thickness solidified, S , against time, t , presented in the form of a t/S against S graph, from which the parameter β (used to calculate h_i) is extracted as an intercept.

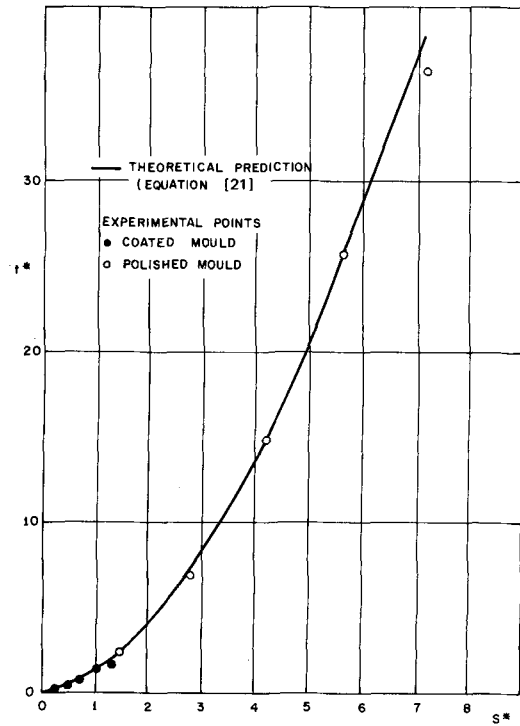


Fig. 6—Comparison between experimental and theoretical dependence of the dimensionless thickness solidified on dimensionless time, with data presented from both polished and coated mold experiments for lead freezing against a semi-infinite mold.

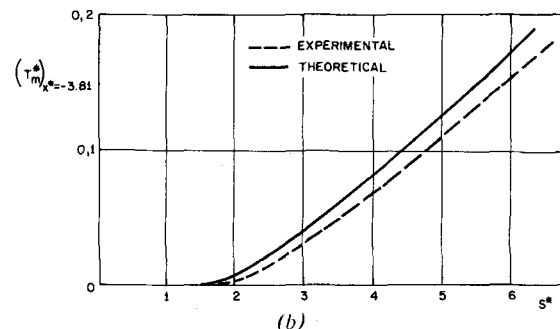
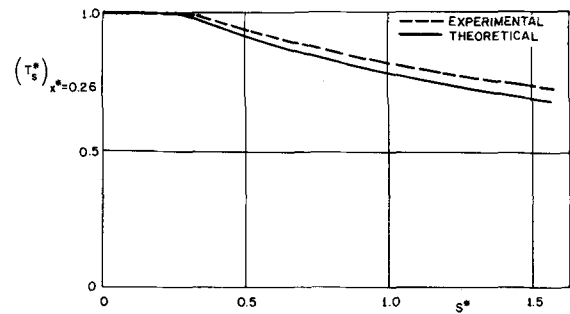


Fig. 7—Comparison between theory and experiment for the thermal history of points in metal and mold variation of temperature with thickness solidified (a) in metal 10 mm from metal/mold interface ($x^* = 0.26$) for coated case and (b) in mold 30 mm from interface ($x^* = -3.81$) for polished case. Experimental curves from thermocouple outputs (combined with appropriate t/S curve): theoretical curves from Eq. [17].

Table II. Values of Parameters Involved in Model Calculated from Data of Table I and Appendix II

Mold Surface	h_i , kJ/m ² ·K·s	N	M	ϕ	T_i , K	h_{is} , kJ/m ² ·K·s	h_{im} , kJ/m ² ·K·s	S_o , mm	E_o , mm
Polished	4.2	1.57	0.58	0.59	447	8.26	8.54	3.1	1.7
Coated (100 μ m)	0.75	1.57	0.58	0.59	447	1.47	1.53	17.1	9.7

practical difficulties associated with the massive mold case.

The effect of a finite mold thickness was also investigated in a short series of experiments with polished mold surfaces. For the 100 mm mold it was verified that the temperature increase of the extremity remote from the metal was negligibly small during the solidification period, but for the other thickness utilized, this increase was significant, indicating some reduction in the heat-extracting efficiency of the mold and consequent deviation from the conditions of the semi-infinite model. The variations in observed t/S relationships for the different mold thickness used are illustrated in Fig. 8. It may be noted that interpolation of these curves indeed indicates that the 100 mm case closely represents a limiting semi-infinite case. Experimentally observed changes of T_{is} with time for these molds, shown in Fig. 9, illustrate this point and also show that with thin molds a temperature reversion may occur at the interface if the heat flux into the mold becomes sensibly lower than that arriving from the body of the metal (*i.e.* if the mold effectively becomes saturated with heat). In practice this will depend on exactly what is happening at the

external surface, as well as on thickness and material of mold.

CONCLUSION

The proposed model is seen to predict quite efficiently the kinetics and thermal characteristics of the solidification process under the conditions examined. Experimentally, the massive mold case is not simple to simulate under the imposed limitations, and agreement between theory and experiment may be considered very good under these circumstances.

Taken in conjunction with the success of the similarly derived model for the case of cooled molds, this clearly indicates the validity of the approach of replacing interfacial resistance with a "pre-existing" thickness of material, through which heat flow obeys the laws of conduction. This rationale would appear to provide a mathematically exact way of treating the generalized solidification problem subject to the restriction that the heat transfer coefficient is an invariant (and leaving aside temporarily the effect of superheat). The analysis combines the advantages of generality and relative simplicity and requires little numerical computation.

It appears probable that a number of practical solidification situations would be amenable to solution by application of the basic idea, subject to some simple physical approximations. For example, in a one- or two-dimensional form the treatment might be applied at a series of positions to continuous casting of narrow freezing range alloys, for which the variation of h_i along the solidifying strand is specified or may be found. Suitable manipulation of the model could enable deductions to be made about the interfacial profile in

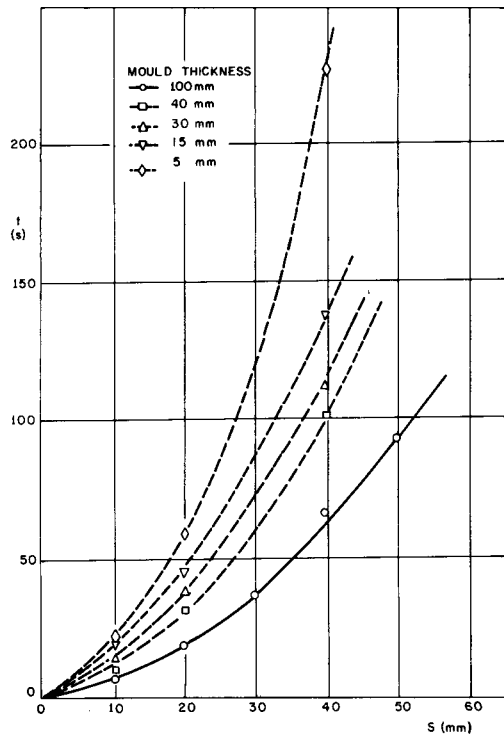


Fig. 8—Experimental measurements of thickness solidified against time for solidification of lead against polished molds of varying thickness.

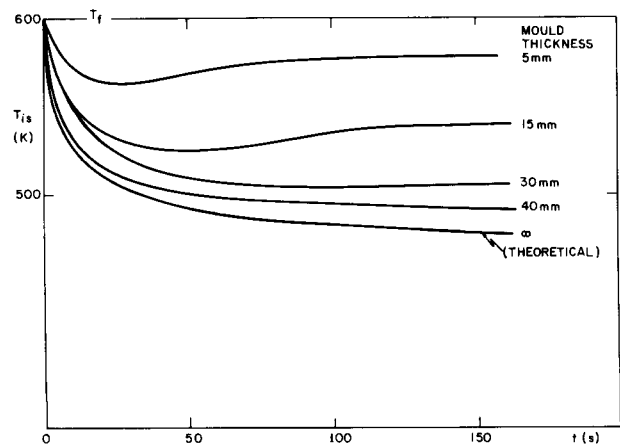


Fig. 9—Experimentally observed cooling curves of metal at the metal/mold interface for solidification of lead against polished molds of varying thickness.

the steady state set up under given conditions. The generality of the description is of value for such applications because thermal measurements made at various locations can be compared with the model predictions.

It may also be noted that the analysis outlined in this paper includes a rapid and convenient method for experimental measurement of heat transfer coefficients. The agreement observed between values obtained in this way for the same materials and surface conditions in both massive and cooled molds provides confirmation of the reliability of this technique.

APPENDIX I. LIST OF SYMBOLS

a) Dimensional Variables and Parameters

a_m	thermal diffusivity of mold material (= $k_m/c_m d_m$), m^2/s ,
a_s	thermal diffusivity of solid metal (= $k_s/c_s d_s$), m^2/s ,
A_m	first integration constant of thermal profile in mold, K,
A_s	first integration constant of thermal profile in metal, K,
B_m	second integration constant of thermal profile in mold, K,
B_s	second integration constant of thermal profile in metal, K,
c_m	specific heat of mold material, J/kg · K,
c_s	specific heat of solid metal, J/kg · K,
d_m	density of mold material, kg/m^3 ,
d_s	density of solid metal, kg/m^3 ,
E_o	thickness of "pre-existing" adjunct to mold in virtual system, m,
h_i	Newtonian heat transfer coefficient of metal/mold interface, $J/m^2 \cdot K \cdot s$,
h_{im}	heat transfer coefficient on mold side of metal/mold interface, $J/m^2 \cdot K \cdot s$,
h_{is}	heat transfer coefficient on metal side of metal/mold interface,
H	latent heat of fusion of metal, J/kg,
k_m	thermal conductivity of mold material, $J/m \cdot K \cdot s$,
k_s	thermal conductivity of solid metal, $J/m \cdot K \cdot s$,
S	thickness of solidified metal in real system, m,
S'	thickness of solidified metal in virtual systems, m,
S_o	thickness of "pre-existing" adjunct to metal in virtual system, m,
t	time from zero point in real system, s,
t'	time from zero point in virtual systems, s,
t_o	time to produce "pre-existing" adjuncts in virtual systems, s,
T	absolute temperature in real and virtual systems, K,
T_f	freezing temperature of metal, K,
T_i	invariant temperature of hypothetical plane at metal/mold interface, K,
T_{im}	temperature of mold at metal/mold interface, K,
T_{is}	temperature of metal at metal/mold interface, K,
T_m	temperature at any point in the mold, K,

T_o	initial temperature of massive mold (ambient temperature), K,
T_s	temperature at any point in the solidified metal, K,
V	velocity of liquid/solid interface in real system, m/s,
x	distance from metal/mold interface in real system, m,
x'	distance from metal/mold interface in virtual systems, m,
α	first constant of Eq. [6] (= $1/4 a_s \phi^2$), s/m^2 ,
β	second constant of Eq. [6] (= $S_o/2a_s \phi^2$), s/m .

b) Dimensionless Variables and Parameters

E_o^*	dimensionless thickness of "pre-existing" adjunct to mold, $E_o h_i/k_m$,
H^*	dimensionless latent heat of fusion of metal, $H/c_s(T_f - T_o)$,
M	ratio of heat diffusivities of solid metal and mold material, $(k_s d_s c_s/k_m d_m c_m)^{1/2}$,
N	square root of ratio of thermal diffusivities of solid metal and mold material, $(a_s/a_m)^{1/2}$,
S^*	dimensionless thickness of solidified metal in real system, Sh_i/k_s ,
S_o^*	dimensionless thickness of "pre-existing" adjunct to metal, $S_o h_i/k_s$,
t^*	dimensionless time from zero point in real system, $th_i^2/k_s d_s c_s$,
T_m^*	dimensionless temperature at any point in the mold, $(T_m - T_o)/(T_f - T_o)$,
T_s^*	dimensionless temperature at any point in the metal, $(T_s - T_o)/(T_f - T_o)$,
$x^*(x > 0)$	dimensionless distance into metal from metal/mold interface, xh_i/k_s ,
$x^*(x < 0)$	dimensionless distance into mold from metal/mold interface, xh_i/k_m ,
ϕ	dimensionless solidification constant, Eq. [20].

Appendix II. Thermal Properties of Metal and Mold Used in Calculation of Model Parameters.

Material	H , kJ/kg	k , J/m · K · s	d , Mg/m ³	c , J/kg · K	T_f , K	T_o , K
Lead	25	31	11.1	138	600	—
Low alloy Steel (En 27)	—	33	7.9	486	—	300

ACKNOWLEDGMENTS

The authors would like to thank FINEP (Brazilian Agency for Research and Development) for providing financial support and Miss Rita Buso for helping with the experimental work.

REFERENCES

1. A. Garcia and M. Prates: *Met. Trans. B*, 1978, vol. 9B, p. 449.
2. H. Jones: *J. Inst. Metals*, 1969, vol. 97, pp. 38-43.
3. R. A. Mizikar: *Trans. TMS-AIME*, 1967, vol. 239, pp. 1747-53.
4. A. W. D. Hills and M. R. Moore: *Trans. TMS-AIME*, 1969, vol. 245, pp. 1481-92.
5. A. W. D. Hills and S. L. Malhotra: *Met. Trans. B*, 1975, vol. 6B, pp. 131-42.

6. F. Megerlin: Ph.D. Thesis, Aachen, Germany, 1966.
7. J. G. Henzel and J. Keverian: *J. AFS*, 1960, vol. 62, pp. 373-79.
8. A. W. D. Hills: *J. Iron Steel Inst.*, 1965, vol. 203, pp. 18-26.
9. R. W. Ruddle: *The Solidification of Castings*, p. 166, Inst. of Metals, London, 1967.
10. G. H. Geiger and D. H. Poirier: *Transport Phenomena in Metallurgy*, p. 346, Addison-Wesley Inc., New York, 1973.
11. C. M. Adams: *Thermal Considerations in Freezing*, p. 187, Liquid Metals and Solidification, Cleveland, 1958.
12. G. Sciama: *Fonderie*, 1968, vol. 268, p. 267.
13. O. S. Pires, M. Prates, and H. Biloni: *Z. Metall. Kd.*, 1974, vol. 65, pp. 143-49.
14. M. Prates and H. Biloni: *Met. Trans.*, 1972, vol. 3, pp. 1501-10.
15. A. Morales, M. E. Glicksman, and H. Biloni: *The Influence of Mould Wall Microgeometry on Casting Structure*, Proceedings Sheffield International Conference on Solidification and Casting, 1977.